# Experimental Study of a Schwedler Rigid Framed Dome

JAMES E. BEAVERS AND FRED BEAUFAIT

THE STEEL FRAMED dome has become quite popular in recent years for use as a roof structure. This popularity is due to the fact that the dome can cover large areas with a minimum amount of material, is free of interior supports, is relatively easy to fabricate and erect, and has a pleasing appearance.

One of the more widely constructed domes is the Schwedler dome[6] shown in Fig. 1. It has a simple geometry and, by assuming pin-connected joints for the structure, can be analyzed for axis-symmetrical loading conditions using the basic equations of statics. The static analysis of the Schwedler dome has been the subject of some research[3,7] and has been presented by AISC.[4] If the joints were assumed to be rigid, analysis would be more difficult, because the model would represent a space frame with a very high degree of indeterminancy. In most instances the joints of a Schwedler dome are better described as rigid, rather than pin-connected, which raises a question about the accuracy of the static analysis. A more sophisticated analysis should be used to properly analyze such a structure.

Currently, only limited experimental and theoretical information is available concerning the response and analysis of rigid steel framed domes.

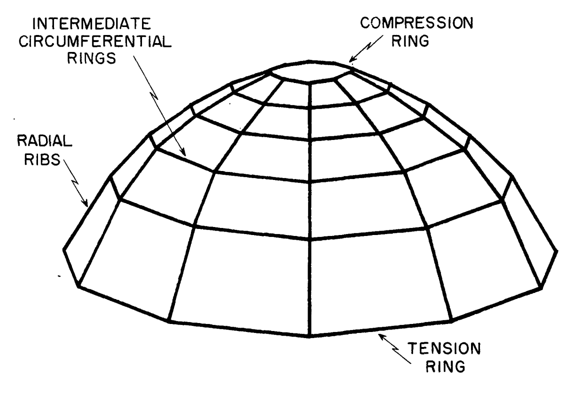


*Fig. 1. Geometrical configuration of a Schwedler dome*

*James E. Beavers is a Graduate Student, Department of Civil Engineering, Vanderbilt University, Nashville, Tenn.*

*Fred W. Beaufait is Associate Professor of Civil Engineering, Vanderbilt University, Nashville, Tenn.*

## OBJECTIVE

The general objective of the investigation discussed in this paper was to conduct and compare the results of an experimental and theoretical study of a steel-framed dome having rigid joints. Specifically, the objectives were (a) to construct a laboratory-size Schwedler steel framed dome with rigid joints that could be subjected to various loadings, both symmetrical and unsymmetrical, (b) to analyze the symmetrically loaded dome using static analyses as presented by AISC, (c) to utilize the stiffness method in conjunction with the computer to analyze the dome structure as a rigid frame, and (d) to compare the analytical and experimental results to evaluate the analysis of the Schwedler framed dome with rigid joints by statics as well as by the stiffness method.

## EXPERIMENTAL PROCEDURES

**Dome description**—The laboratory-size Schwedler dome used in this study was constructed of A36 steel. It had twelve radial ribs and six circumferential rings and rested on a rigid support frame, as shown in Fig. 2. The total number of members was 132 and the total number of joints was 72.

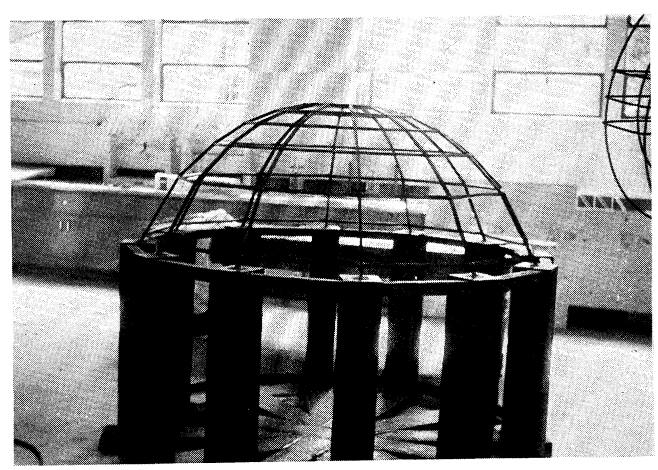

*Fig. 2. Laboratory Schwedler dome and support frame*

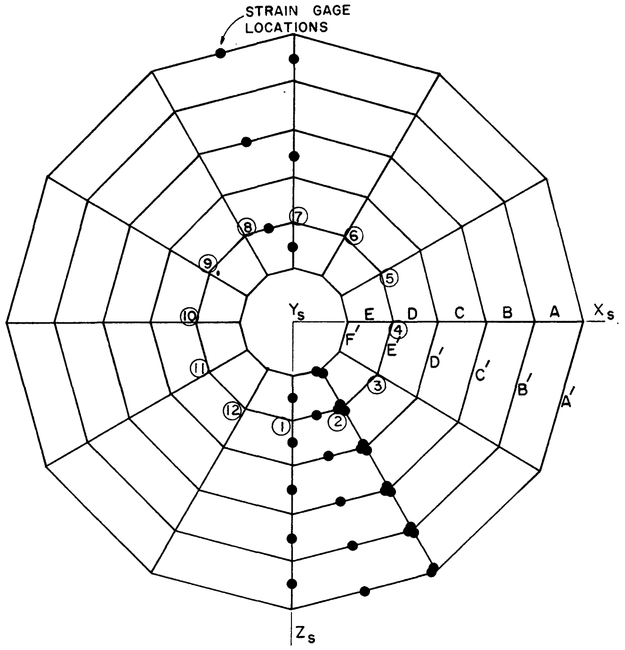


*Fig. 3. Plan view of experimental dome, showing member notation, joints to be loaded, and strain gage locations*

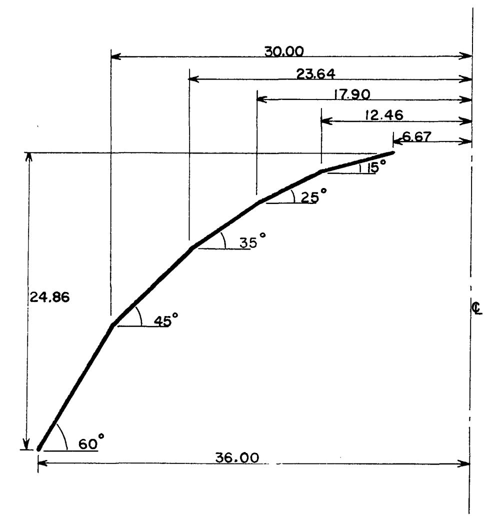


*Fig. 4. Experimental dome rib profile; dimensions in inches*

The ribs, members **A, B, C, D,** and **E** in Fig. 3, were constructed of ½-in. square bars. The lower two rings, members **A′** and **B′**, were also constructed of ½-in. square bars. The remaining four rings, members **C′, D′, E′,** and **F′**, were constructed of ⅜-in. square bars. The members were welded together, forming a condition of rigid joints. Individual member geometry is given in Table 1.

**Table 1. Member Geometric Properties**

| Member | Length (in.) | Area (in.$^2$) | Moment Inertia (in.$^4$ $\times$ $10^{-3}$) | Angle of Twist[a] (degrees) |
|---|---|---|---|---|
| A | 12.00 | 0.250 | 5.21 | 0.0 |
| B | 9.00 | 0.250 | 5.21 | 0.0 |
| C | 7.00 | 0.250 | 5.21 | 0.0 |
| D | 6.00 | 0.250 | 5.21 | 0.0 |
| E | 6.00 | 0.250 | 5.21 | 0.0 |
| A′ | 18.68 | 0.250 | 5.21 | 60.0 |
| B′ | 15.52 | 0.250 | 5.21 | 60.0 |
| C′ | 12.20 | 0.141 | 1.65 | 45.0 |
| D′ | 9.24 | 0.141 | 1.65 | 35.0 |
| E′ | 6.45 | 0.141 | 1.65 | 25.0 |
| F′ | 3.46 | 0.141 | 1.65 | 15.0 |

[a] Angle of twist is the angle between the member's $x$-$y$ plane and the structure's $x$-$y$ plane, measured in the member's $y$-$z$ plane when the right end of the member is looked upon from outside the dome's circumference moving in a counter-clockwise direction (Fig. 3).

The base of the dome was essentially 72 in. in diameter and the dome had a rise of 24.86 in. from the bottom tension ring **A′** to the top compression ring **F′**. The dome had a clear opening at the top of 13.34 in.

The rib geometry is shown in Fig. 4; it is symmetrical about the dome's center line. At the base of each rib a support was constructed that permitted the dome to expand in a radial direction, but these supports were later welded to the supporting frame for accommodation of analyses. The supports were constructed by welding flat plates to the bottom of a short extension of the rib; these plates rested on top of a supporting column (Fig. 2).

**Loading Technique**—The loads were applied to selected joints on the dome by a system of tie rods, shown in Fig. 5. Two chain links were welded to the selected joints and high strength rods were attached to the lower end of the bottom chain link (Fig. 5a). The lower end of the rods was threaded and extended through slots which had been cut into the base of the support frame (Fig. 5b). Thus, downward loads could be applied to the joints by adjusting taps, threaded onto the tie rods, against the bottom side of the support frame base. The chain links were used to avoid developing moments at the joints that might be caused by the tie rods. The loads were applied to the dome at the joints of ring **E′**, which are identified by the encircled numbers shown in Fig. 3. The symmetrical load applied to the structure was 500 lbs at each joint of ring **E′** and the unsymmetrical load was 600 lbs applied at only one selected joint of ring **E′**.

(*a*) *Upper connection*

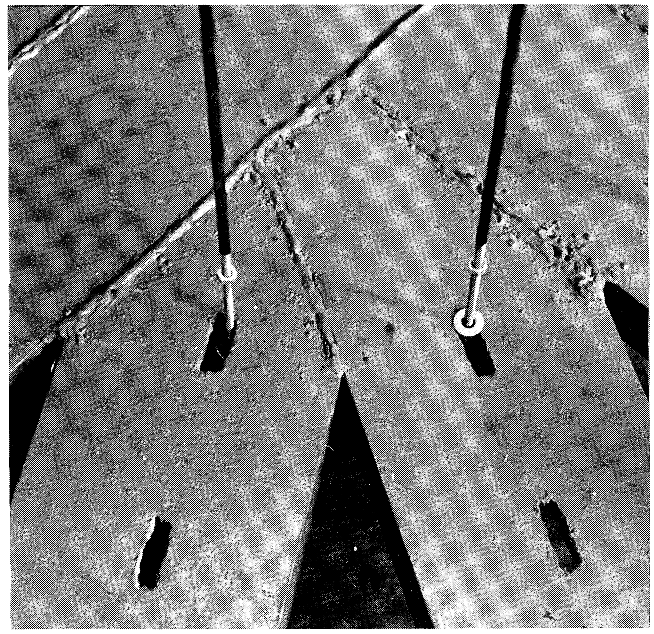

(*b*) *Lower connection*

*Fig. 5. Loading rod system*

**Instrumentation**—SR4 Type A-7 strain gages were used to measure the response of the dome at selected locations and the loads produced at the joints by the tie rods. One gage was placed on the top side and another on the bottom side of a member at each selected location of the dome shown in Fig. 3, to enable the determination of axial forces and moments produced in the system by the applied loads. Two strain gages were placed diametrically opposite each other on the tie rods to obtain an average strain measurement and thus the applied load. The strains were recorded using SR4 Strain Indicators.

## ANALYTICAL ANALYSES

**Static Analyses**—Static analyses of steel framed domes have been presented by Anderson and Graves[1], Anderson[2,3], Stevens and Odom[7], and the AISC.[4] In order to use a statics analysis for a Schwedler dome, the required criteria is that the joints must be pinned. This method of analysis can easily be used for symmetrical loadings in that only the joints of one rib of the dome need be analyzed. If this method were used to analyze the structure for an unsymmetrical loading, every joint of a structure would have to be considered; such an analysis has been found to give erroneous results.[7] Thus, the experimental dome was analyzed using the equations of statics for only a symmetrical loading, with the assumptions that the joints were pinned, to investigate the magnitude of error that might have developed using this static analysis for such a structure.

**Stiffness Method and Code**—The stiffness method enables the practicing engineer to analyze rigid space frames having very large degrees of indeterminancy. Its fundamental equations are derived by using the principal of superposition with the unknown quantities in the analysis being the unrestrained joint displacements (translations and rotations). The mechanics of this method of analysis and the computer programming procedures are thoroughly presented in Ref. 5 and are not the concern of this paper.

## RESULTS

**Symmetrically Loaded Dome**—Shown in Figure 6 is a comparison of member axial forces and end moments determined experimentally by the Schwedler (static) analysis and by the stiffness analyses for a symmetrically loaded dome.

Symmetrical load tests were performed with the base plates fixed, to be compared to the stiffness analysis, and also with them free to expand radially, to be compared to the static analysis. The magnitudes of the axial forces in the members did not change greatly between having the base plates fixed or free except for ring **A′**, in which these forces were reduced greatly when the base plate was fixed to the support, as might be expected. The stiffness analysis shows the magnitude of the axial force in ring **A′** as 13 lbs, compared to 168 lbs determined experimentally with the base fixed. The loading of ring **A′** was caused by a small initial outward movement of the support frame which occurred when the

**Table 2. Symmetrical Load Case[a,b,c,d]**

| Member (See Fig. 3) | Experimental | | | Schwedler (Static) Analysis | Stiffness Analysis (End Actions) | | | | | |
|---|---|---|---|---|---|---|---|---|---|---|
| | $P_x$[e] (lbs) | $P_x$[f] (lbs) | $M_z$[f] (in.-lbs) | $P_x$ (lbs) | $P_x$ (lbs) | $P_y$ (lbs) | $P_z$ (lbs) | $M_x$ (in.-lbs) | $M_y$ (in.-lbs) | $M_z$ (in.-lbs) |
| A′ | −471 | −168 | 0 | −557 | −13 | 0 | 0 | 0 | 0 | 0 |
| B′ | −344 | −355 | 4 | −408 | −400 | 0 | 0 | 0 | 0 | 0 |
| C′ | −489 | −467 | 2 | −416 | −489 | 0 | 0 | 0 | 0 | 0 |
| D″ | −426 | −376 | −14 | −688 | −341 | 0 | 0 | 0 | −4 | 5 |
| E′ | 1547 | 1361 | −70 | 2070 | 1482 | 0 | 0 | 0 | −1 | 2 |
| F′ | 552 | 543 | −40 | 0 | 308 | 0 | 0 | 0 | 7 | −27 |
| A | 610 | 609 | 3 | 557 | 578 | −1 | 0 | 0 | 0 | 6 |
| B | 721 | 636 | −32 | 707 | 705 | 2 | 0 | 0 | 0 | −5 |
| C | 1000 | 842 | 1 | 874 | 901 | −21 | 0 | 0 | 0 | 14 |
| D | 987 | 916 | −115 | 1182 | 1051 | 61 | 0 | 0 | 0 | −135 |
| E | 173 | 166 | 180 | 0 | 153 | −41 | 0 | 0 | 0 | 233 |

[a] 500-lb load at each joint of ring E′.
[b] A negative axial force is a tensile force and a negative moment causes tension in the top surface.
[c] The moment values shown are the moments at the lower joint of rib members and the right end of ring members (Fig. 3).
[d] A member free-body diagram is shown in Fig. 6.
[e] Base plate free to expand radially.
[f] Base plate fixed.

loads were initially applied to the dome and which would naturally affect ring **A′** more than other members, due to the geometrical configuration.

Overall, the Schwedler analysis is in general agreement, as to the magnitudes of the axial forces, with the experimental results and the results of the stiffness analysis. The disagreement with respect to the magnitudes of the axial forces in ring **D′**, **E′** and **F′**, and rib **E**, results from the assumption of pinned joint conditions in the Schwedler analysis, which would not indicate any transmission of forces to ring **F′** or rib **E′**, thus predicting larger forces to be carried by rings **D′** and **E′**, as shown in Table 2. The stiffness analysis is much more accurate in predicting the force distributions during the experimental testing of the dome subjected to the symmetrical loads. This analysis does show that forces were transmitted, by the rigidity of the joints, to rib **E** and ring **F′**, which resulted in a reduction of the forces incurred by rings **D′** and **E′**.

The moment comparisons between the experimental results and stiffness analysis agree reasonably well for magnitudes greater than 100, while those of smaller magnitude show some wide variations. The smaller magnitude moments are naturally much more susceptible to possible accumulative experimental errors.

**Unsymmetrically Loaded Dome**—Tables 3 and 4 show comparisons between the experimental results and stiffness analysis of the axial forces and end moments for two unsymmetrical load cases: one for a single load at joint **1** and the other for a single load at joint **3**, respectively. In comparing the experimental results with the stiffness analysis it can be seen that there is good agreement as to the magnitudes of the axial forces in the members. Since the dome rib containing members **79, 80, 81, 82,** and **83** lies between the dome ribs containing joints **1** and **3**, the forces produced in this rib by a load at joint **1** will be identical to those produced by the same load at joint **3** due to geometric symmetry. By examining the axial forces of these members, shown in Tables 3 and 4 for both symmetrical loadings, it can be seen that the stiffness analysis readily reveals the symmetry condition with considerable accuracy. The experimental results indicate that the condition of sym-

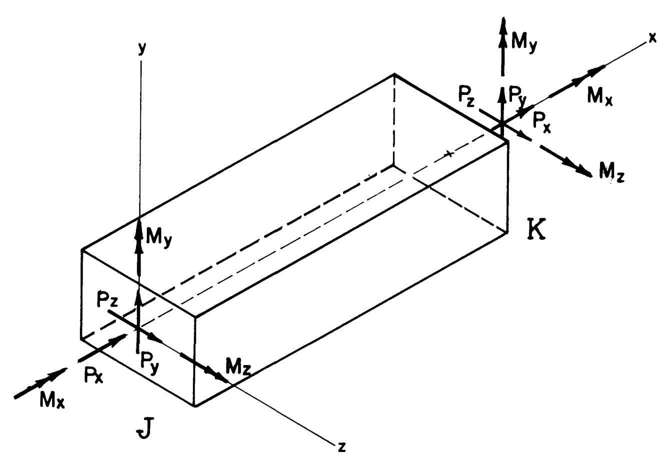


*Fig. 6. Member free-body diagram*

**Table 3. Unsymmetrical Load Comparison Load at Joint 1 (600 lbs)**

| Member (See Fig. 7) | Experimental | | | Stiffness Analysis (End Actions) | | | | | | | | |
|---|---|---|---|---|---|---|---|---|---|---|---|---|
| | $P_xJ^{a,b}$ (lbs) | $M_xJ$ (in.-lbs) | $M_zK$ (in.-lbs) | $P_xJ$ (lbs) | $P_yJ$ (lbs) | $P_zJ$ (lbs) | $M_xJ$ (in.-lbs) | $M_yJ$ (in.-lbs) | $M_zJ$ (in.-lbs) | $M_xK$ (in.-lbs) | $M_yK$ (in.-lbs) | $M_zK$ (in.-lbs) |
| 1 | −18 | | 2 | −18 | 0 | 1 | −9 | −7 | −5 | −9 | 6 | 3 |
| 13 | −105 | | 87 | −76 | 14 | 4 | −3 | 42 | −107 | −3 | −21 | 110 |
| 25 | −67 | | 58 | −61 | 6 | 13 | −23 | −82 | 8 | 23 | −73 | 61 |
| 37 | −14 | | 7 | −14 | −17 | 25 | −46 | −126 | −145 | 47 | −106 | −7 |
| 49 | 285 | | −108 | 309 | −88 | 18 | −4 | −70 | −394 | 4 | −45 | −175 |
| 61 | −50 | | 15 | 9 | −61 | −57 | 72 | 116 | −265 | −72 | 81 | 54 |
| 74 | 261 | | | 331 | 24 | 0 | 0 | −3 | 214 | 0 | −3 | 79 |
| 75 | 326 | | | 369 | −9 | 1 | 0 | −2 | 112 | 0 | −2 | −201 |
| 76 | 395 | | | 414 | −49 | 0 | 0 | −2 | −161 | 0 | 0 | −185 |
| 77 | 344 | | | 449 | −159 | 0 | 0 | −2 | −927 | 0 | 0 | −28 |
| 78 | 62 | | | 111 | 122 | 0 | 0 | −1 | 20 | 0 | 0 | 717 |
| 79 | −32 | −138 | 205 | 10 | 10 | 54 | 35 | −137 | −125 | −35 | −189 | 184 |
| 80 | 116 | −203 | 92 | 130 | −14 | −55 | 143 | 282 | −172 | −143 | 45 | 86 |
| 81 | 134 | −72 | −13 | 118 | −13 | −48 | 123 | 216 | −77 | −123 | 119 | −12 |
| 82 | — | −3 | −74 | 91 | −9 | −28 | 60 | 94 | −5 | −60 | 159 | −75 |
| 83 | 62 | 30 | −74 | 63 | −4 | −1 | −10 | −5 | 25 | 10 | 20 | −74 |

[a] Axial force at *K*-end is equal and opposite to the axial force at the *J*-end.
[b] See Fig. 6 for sign convention; force directions shown in Fig. 6 are positive.

**Table 4. Unsymmetrical Load Comparison Load at Joint 3 (600 lbs)**

| Member (See Fig. 7) | Experimental | | | Stiffness Analysis (End Actions) | | | | | | | | |
|---|---|---|---|---|---|---|---|---|---|---|---|---|
| | $P_xJ^{a,b}$ (lbs) | $M_zJ$ (in.-lbs) | $M_zK$ (in.-lbs) | $P_xJ$ (lbs) | $P_yJ$ (lbs) | $P_zJ$ (lbs) | $M_xJ$ (in.-lbs) | $M_yJ$ (in.-lbs) | $M_zJ$ (in.-lbs) | $M_xK$ (in.-lbs) | $M_yK$ (in.-lbs) | $M_zK$ (in.-lbs) |
| 1 | −51 | | 3 | −7 | −0 | −1 | −3 | 12 | 5 | 3 | 12 | 2 |
| 13 | −62 | | 8 | −55 | −4 | −14 | 11 | 99 | −59 | −11 | 12 | 3 |
| 25 | −188 | | −15 | −49 | −3 | −21 | 21 | 126 | −23 | −21 | 129 | −11 |
| 37 | −8 | | −16 | −17 | 0 | −31 | 37 | 145 | 8 | −37 | 146 | −12 |
| 49 | 124 | | −37 | 198 | 6 | −17 | 38 | 58 | 58 | −38 | 53 | −18 |
| 61 | 137 | | 25 | 99 | 64 | 42 | 23 | −86 | 146 | −23 | −60 | 76 |
| 74 | −18 | | | −4 | 15 | 13 | −12 | −95 | 107 | 12 | −66 | 70 |
| 75 | −4 | | | 14 | 0 | 37 | −37 | −195 | −43 | 37 | −136 | 40 |
| 76 | 11 | | | 33 | −11 | 51 | −65 | −119 | −51 | 65 | −238 | −23 |
| 77 | −47 | | | 44 | −12 | 52 | −95 | −49 | −7 | 95 | −265 | −66 |
| 78 | 76 | | | −18 | 8 | −18 | −122 | 101 | −35 | 122 | 8 | 12 |
| 79 | −73 | −141 | 205 | 12 | 9 | 54 | −36 | 137 | −124 | 36 | 189 | 182 |
| 80 | 163 | −178 | 89 | 131 | −14 | −55 | −144 | −285 | −170 | 144 | −45 | 85 |
| 81 | 160 | −61 | −10 | 120 | −13 | −49 | −124 | −220 | −77 | 124 | −120 | −11 |
| 82 | 174 | 5 | −86 | 92 | −9 | −29 | −60 | −98 | −5 | 60 | −163 | −75 |
| 83 | 65 | 44 | −57 | 65 | −4 | −2 | −10 | −1 | 26 | −10 | −26 | −73 |

[a] Axial force at *K*-end is equal and opposite to the axial force at the *J*-end.
[b] See Fig. 6 for sign convention; force directions shown in Fig. 6 are positive.

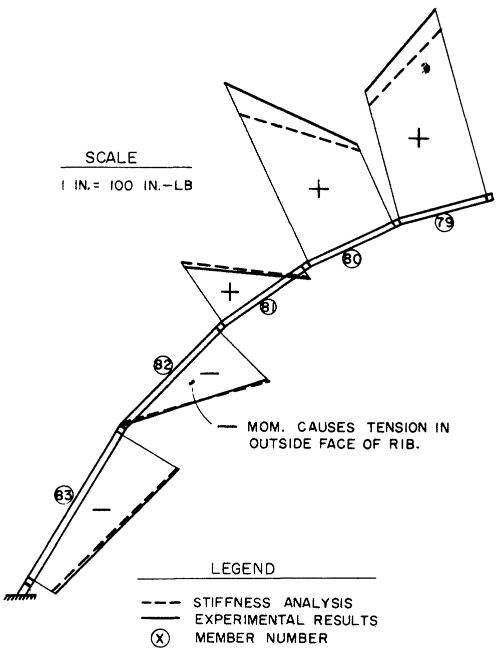


*Fig. 7. Stiffness analysis and experimental result moment diagrams across rib members 79, 80, 81, 82, and 83 with a 600-lb load at joint 1*

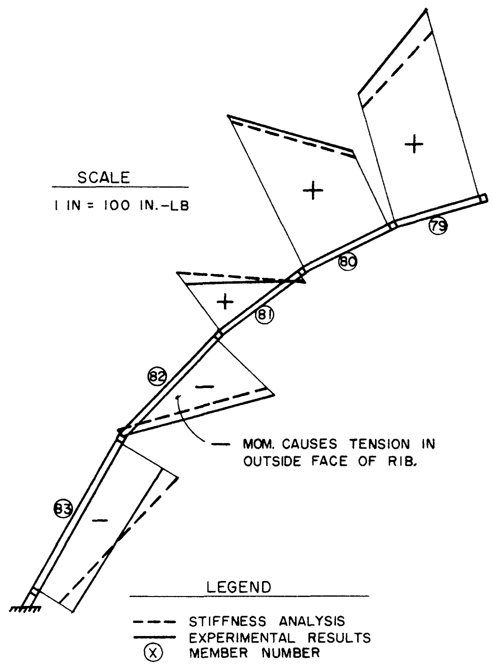


*Fig. 8. Stiffness analysis and experimental result moment diagrams across rib members 79, 80, 81, 82, and 83 with a 600-lb load at joint 3*

metry exists, but not as accurately as the stiffness analysis. The experimental moment magnitudes that were measured for the unsymmetrical load cases do agree reasonably well with those of the stiffness analysis. Shown in Figs. 7 and 8 are moment diagrams across rib members **79, 80, 81, 82,** and **83** for the unsymmetrical load at joints **1** and **3,** respectively, graphically comparing the experimental results with the stiffness analysis. The moment diagrams were constructed using the data of the member end moments (Tables 3 and 4).

## CONCLUSIONS

For symmetrical loading of a Schwedler rigid framed dome, the static analysis yields results that can be used for design purposes; allowance must be made for the fact that this analysis does not consider any bending response of the elements. As indicated by both the experimental study and the theoretical analysis by the stiffness method, bending actions are produced in the frame but are, in general, relatively small in magnitude. For the unsymmetrical loading condition of the Schwedler dome, the experimental study reinforced the findings of earlier studies; a static analysis would yield erroneous results. The bending moments developed within the dome are of significant magnitude and cannot be neglected.

The rigid frame dome can be analyzed by the stiffness method of analysis when programmed for the computer for any desired loading condition, symmetrical or unsymmetrical. The early limitations to this method of analysis is the size of core of the available computer. This could be a serious limitation.

## REFERENCES

1. *Anderson, P., and Graves, W.* Analysis of a Steel Framed Dome *Institute of Technology, University of Minnesota, Minneapolis, Minn., February, 1957.*
2. *Anderson, P.* Stress Study of a Steel Framed Dome *Institute of the National Engineering Conference, American Institute of Technology, University of Minnesota, Minneapolis, Minn., October, 1958.*
3. *Anderson, P.* Steel Framed Domes—Design and Research *Proceedings of the National Engineering Conference, American Institute of Steel Construction, 1959.*
4. Design Examples—Space Forms in Steel *American Institute of Steel Construction, May 1966.*
5. *Beaufait, F. W., et al.* Computer Methods of Structural Analysis *Prentice-Hall, Inc., Englewood Cliffs, New Jersey, 1970.*
6. *Makowski, Z. S.* Steel Space Structures, *Battersea College of Technology, London, England: Michael Joseph, 1964.*
7. *Stevens, D. E. and Odom, G.* The Steel Framed Dome *Engineering Journal, American Institute of Steel Construction, Vol. 1, July, 1964, pp. 83-91.*